CHAPTER IV
RESULTS AND DISCUSSION

4.1 The Catalyst Characterization

4.1.1 Hydrogen Chemisorption

The degree of metal dispersion results obtained on the pellet samples after reduction at either 400°C or 500°C are reported in Table 4.1.

Table 4.1 The degree of metal dispersion characterized by using hydrogen chemisorption measurement.

Type of catalyst	Preparation method	Reduction temperature (°C)	Dispersion (%)
Pt/KL	IWI	500	70.19
Pt/KL	CVD	400	90.31
Pt/KL	CVD	500	70.99
PtYb/KL	CVD	500	80.75

All of catalysts show the high degree of metal dispersion, particularly in the ytterbium promoted catalyst. Interestingly, CVD catalysts exhibited the higher degree of metal dispersion than IWI catalyst. The high reduction temperature resulted in a decrease in dispersion of Pt in zeolite. The sensitivity to high reduction temperature was remarkably observed in IWI catalyst.

4.1.2 Infrared Spectroscopy

The FTIR of adsorbed CO has been widely used to characterize the distribution and location of Pt particles (Lane *et al.*, 1993). The results in this work was consistent with the previous work (Jacobs *et al.*, 1999) that Pt/KL catalyst display complex bands which typically extend from 2080 cm^{-1} to much lower wave number (e.g., as low as 1930 cm^{-1}). The evidence of bands at low wave numbers was explained by EXAFS experiments of Mojet and Koningsberger (1996). They revealed that small Pt particles decomposed upon CO exposure and led to small $[Pt(CO_2)_3]$ entities which were stabilized by the basicity of the zeolite pore walls.

However, the position of band cannot be used directly as an indicator of the dispersion. There are some complications such as electronic effects, dipole-dipole interactions and interaction of CO with the zeolite which can modify the frequencies. Therefore, the extension of the band position to the lower wave number was ascribed from the secondary effects as mentioned above. The interpretations of the results in this work are based on three important regions that were believed to correspond with three variations of morphology of Pt clusters (Stakheev *et al.*, 1995);

(1) Bands below 2050 cm^{-1} are assigned to Pt-CO species arising from the disruption of small Pt clusters inside the L-zeolite channels.

(2) Bands between 2050 and 2075 cm^{-1} are associated with larger Pt clusters in the near-surface region of the L-zeolite.

(3) Bands at around 2080 cm^{-1} are in general assigned to larger Pt particles on the external surface of the L-zeolite.

These informations agree with the results obtained in this study. The variations in the morphology of the catalyst resulted from the different procedures of metal loading are illustrated by the various bands in Figures 4.1 and 4.2. All of them displayed the major band below 2050 cm^{-1} that demonstrated the small Pt clusters inside the channels.

By increasing the reduction temperature to 500°C, the bands around 2050-2075 cm^{-1}, corresponding to the larger Pt cluster in the near-surface region of the L-zeolite were more pronounced. The shift of spectra to high wave number was remarkably observed in the IWI catalyst. Furthermore, the bands around 1970 cm^{-1}, which assigned to the very highly dispersed cluster in zeolite, were more pronounced than that of IWI catalysts.

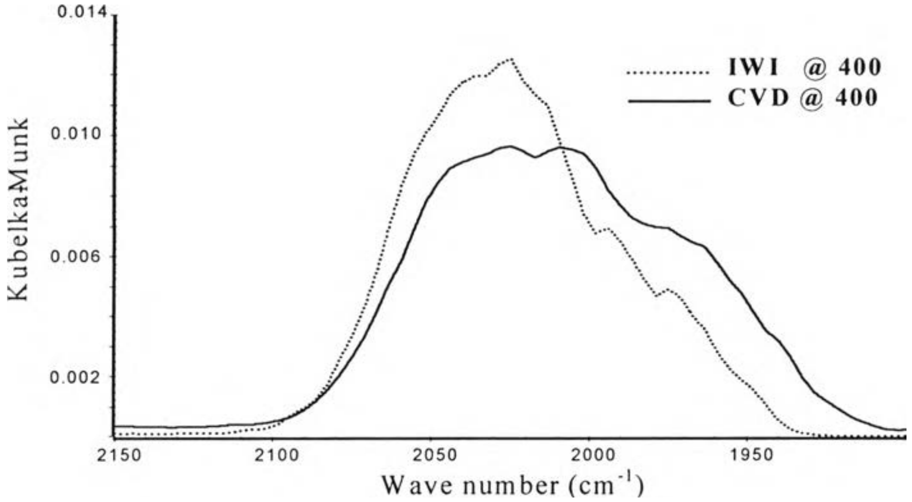

Figure 4.1 The FTIR spectra of adsorbed CO on Pt/KL of IWI and CVD catalysts after reduction at 400 °C.

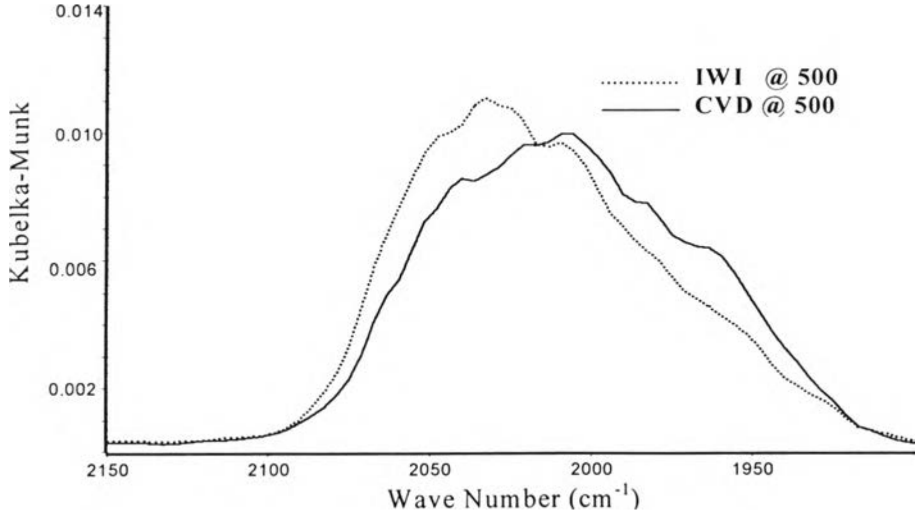

Figure 4.2 The FTIR spectra of adsorbed CO on Pt/KL of IWI and CVD catalysts after reduction at 500 °C.

According to Figures 4.3 and 4.5, the spectra of adsorbed CO in the presence of 0.6 ppm sulfur at 400°C indicated that almost Pt outside the channels were poisoned as shown by the drop of bands in the region 2010 – 1970 cm^{-1}. For distinguishable shoulder around 1930 cm^{-1}, it may have occurred from sulfur poisoning minor amount of Pt inside the channels that probably led to increasing the electron density of support resulted in stabilization of small particles inside the channel. However at high temperature condition, 500°C (Figures 4.4 and 4.6) the spectra displayed the large decreases in the region of 2010 and 1970 cm^{-1}, including the drastically drop in the shoulder between 1950-1930 cm^{-1}. This demonstrated the growth of Pt cluster inside the channels while the major bands extended to the frequencies around 2050 – 2030 cm^{-1} which evidenced the migration of large Pt cluster toward the pore mouth resulting in the partial blockage of channels in the longer reaction time.

By increasing sulfur concentration to 2.5 ppm, the deactivation of catalysts by sulfur poisoning was clearly observed. The band around 1950 – 1930 cm^{-1} disappeared and the greater fractions of bands above 2050 cm^{-1} were distinguished. Their distributions to high wave number in the region of 2080 – 2060 cm^{-1} indicated that major cluster growth to the large cluster which migrated to outside of the channel resulting in loss in its activity and selectivity and the pore mouths blockage.

The stability of ytterbium promoted catalysts to sulfur poisoning was also examined. From the results in Figures 4.7 to 4.12, PtYb/KL showed the higher degree of metal dispersion and lower fraction of the large Pt cluster aggregated out of the pores in comparison with the Pt/KL, CVD catalysts.

The study of thermal treatment by FTIR provided the evidence that catalysts were more stable at lower temperature even in the presence of sulfur. This was confirmed by the shift of spectrum to lower wave number after reduction at 400°C in comparison with after reduction at 500°C.

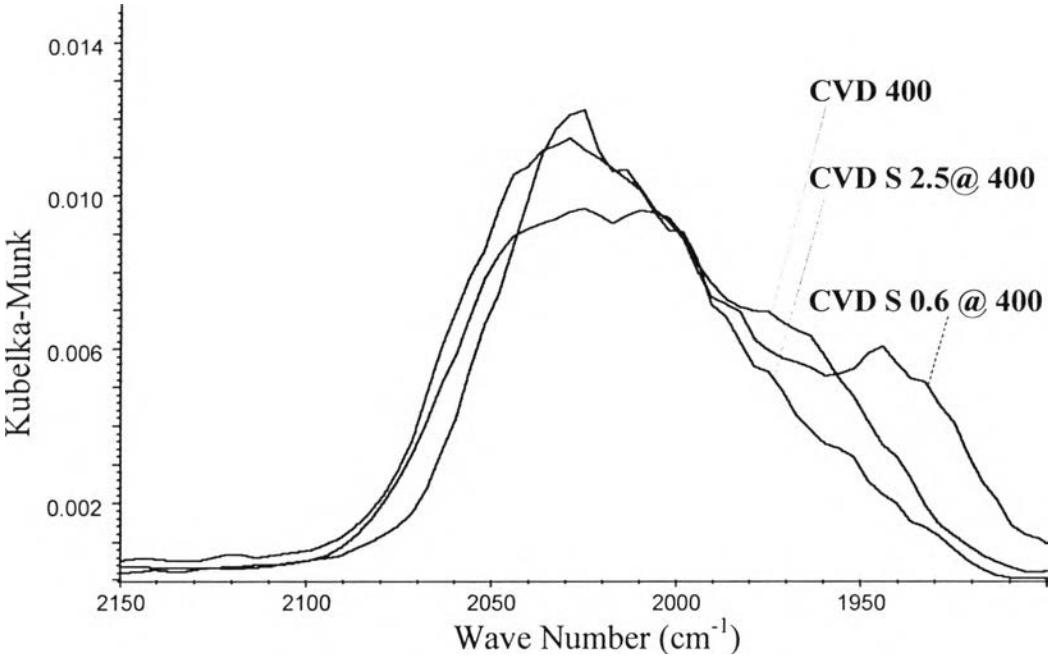

Figure 4.3 The FTIR spectra of adsorbed CO on Pt/KL (CVD method) freshly reduced and after spent in 0.6 and 2.5 ppm sulfur, reduced at 400°C.

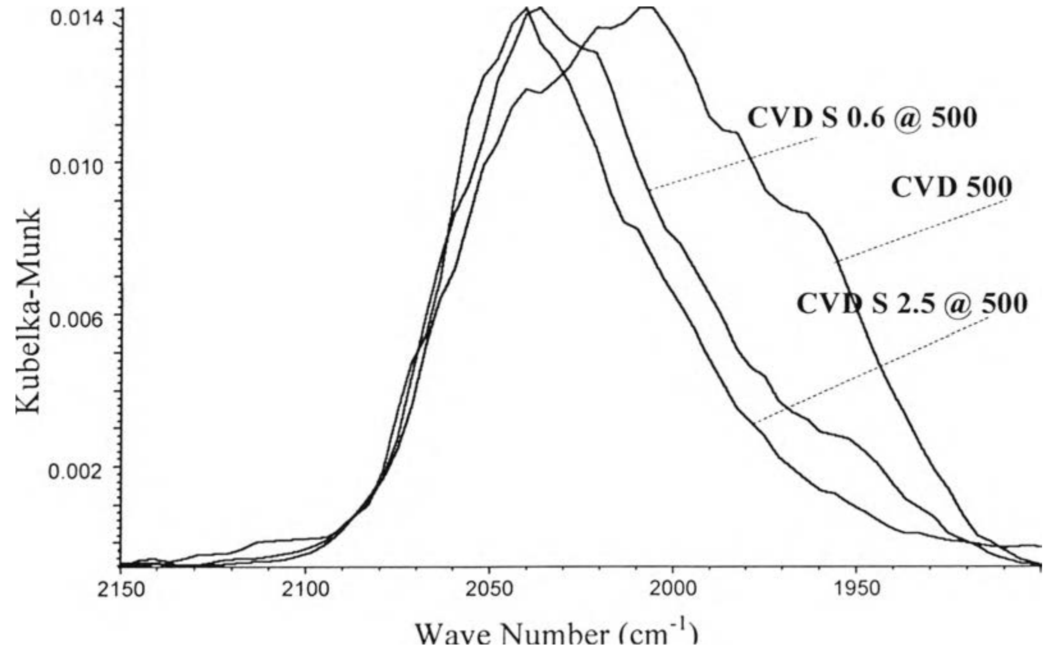

Figure 4.4 The FTIR spectra of adsorbed CO of Pt/KL (CVD method) freshly reduced and after spent in 0.6 and 2.5 ppm sulfur, reduced at 500°C.

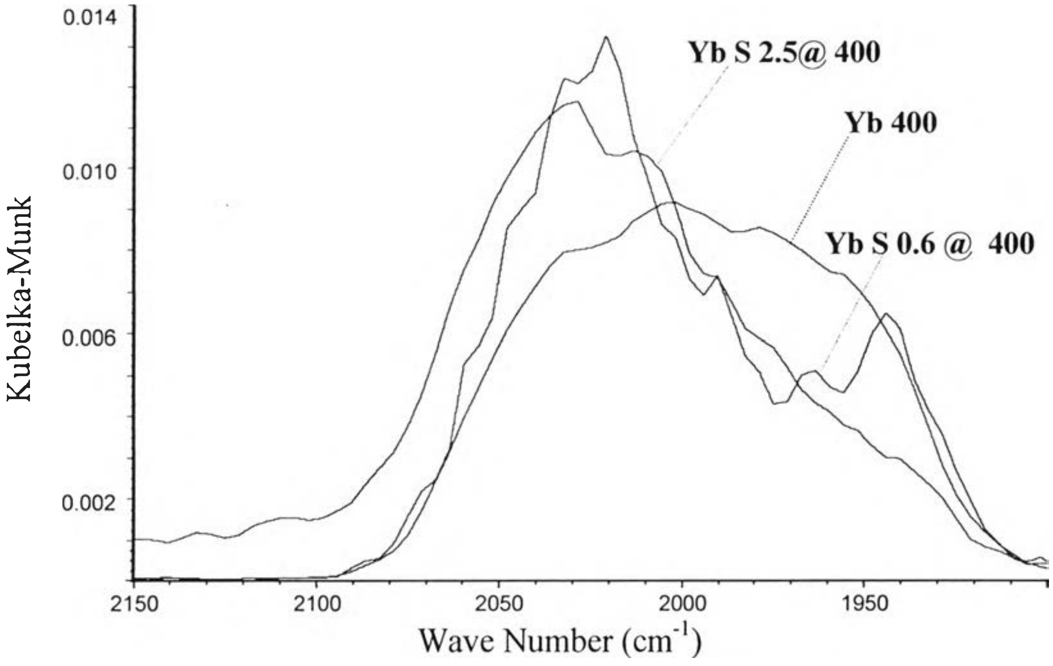

Figure 4.5 The FTIR spectra of adsorbed CO on PtYb/KL (CVD method) freshly reduced and after spent in 0.6 and 2.5 ppm sulfur, reduction at 400°C.

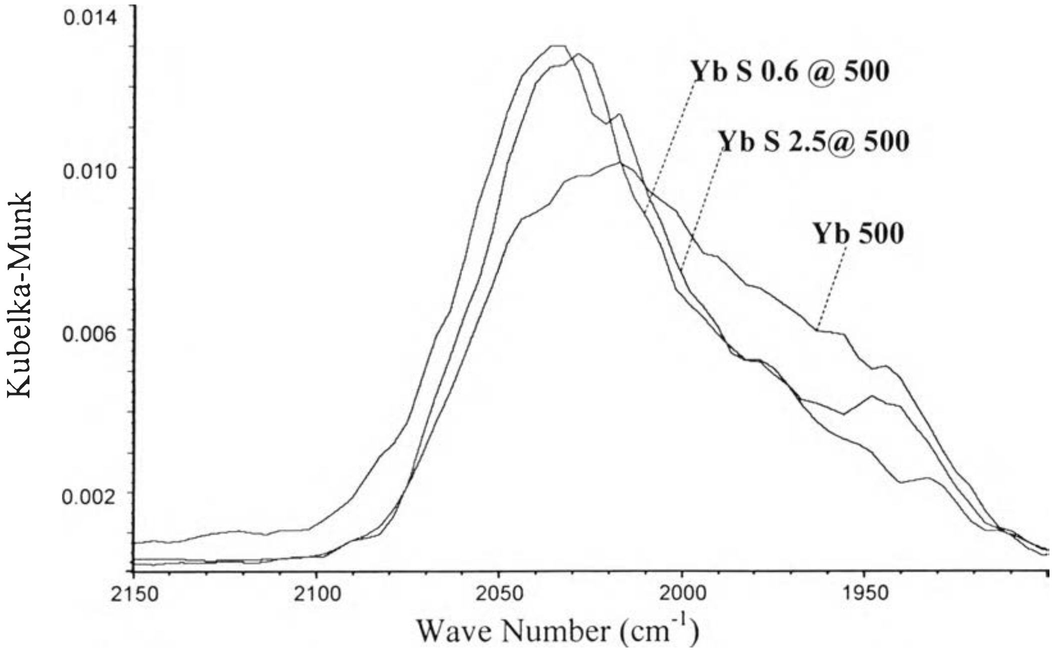

Figure 4.6 The FTIR spectra of adsorbed CO on PtYb/KL (CVD method) freshly reduced and after spent in 0.6 and 2.5 ppm sulfur, reduction at 500°C.

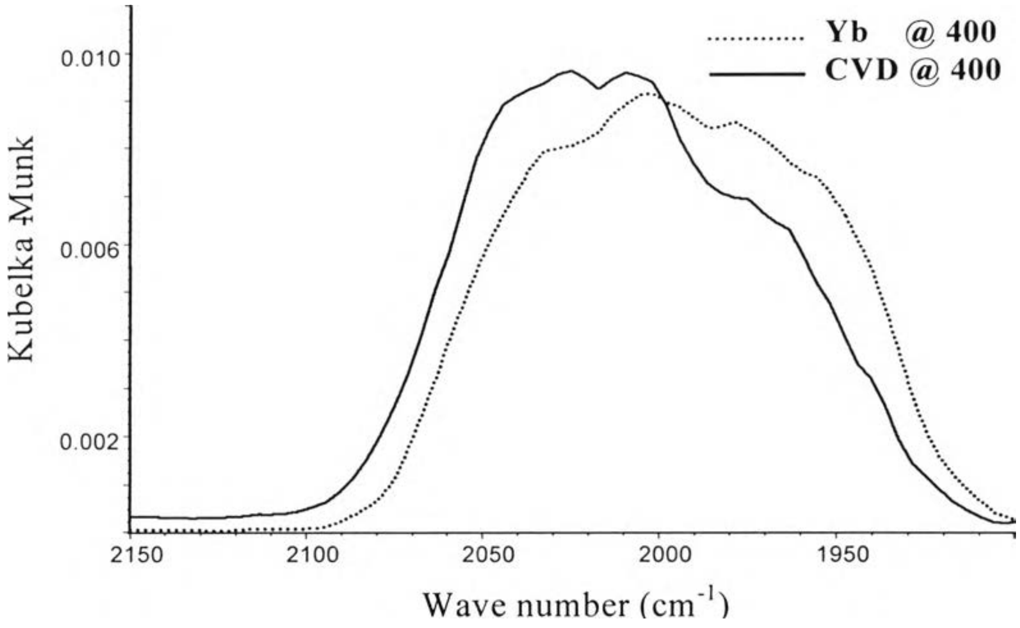

Figure 4.7 The FTIR spectra of adsorbed CO on Pt/KL and PtYb/KL prepared by CVD method after reduction at 400°C.

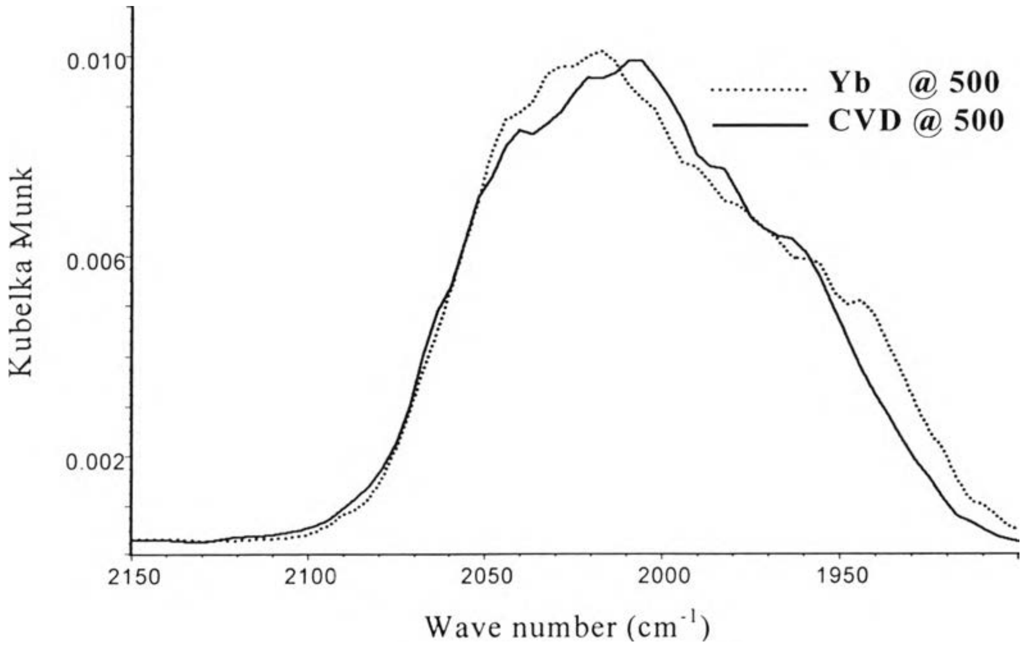

Figure 4.8 The FTIR spectra of adsorbed CO on Pt/KL and PtYb/KL prepared by CVD method after reduction at 500 °C.

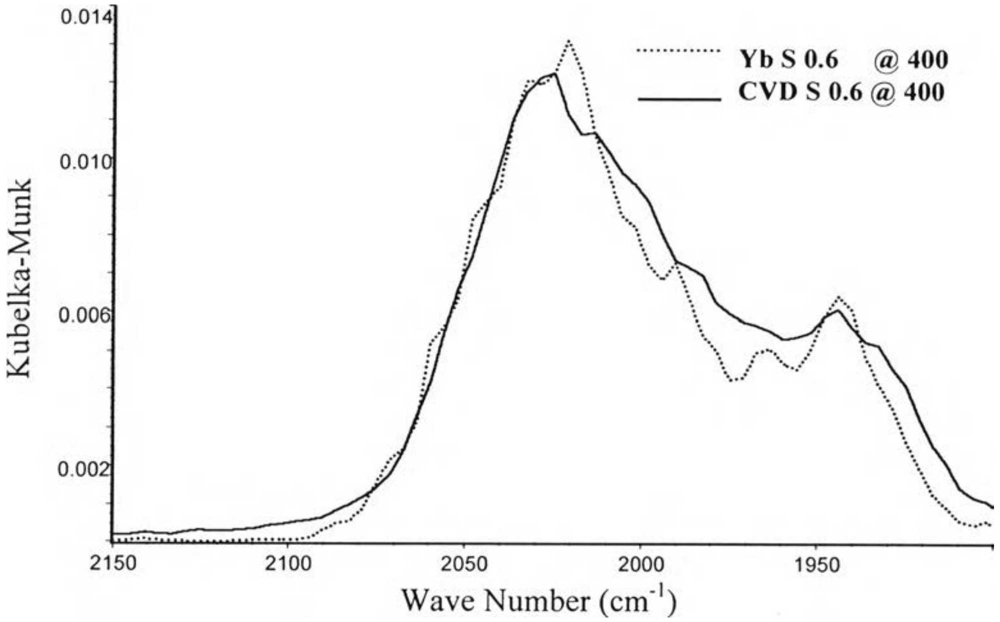

Figure 4.9 The FTIR spectra of adsorbed CO on Pt/KL and PtYb/KL prepared by CVD method after spent in 0.6 ppm sulfur and reduction at 400°C.

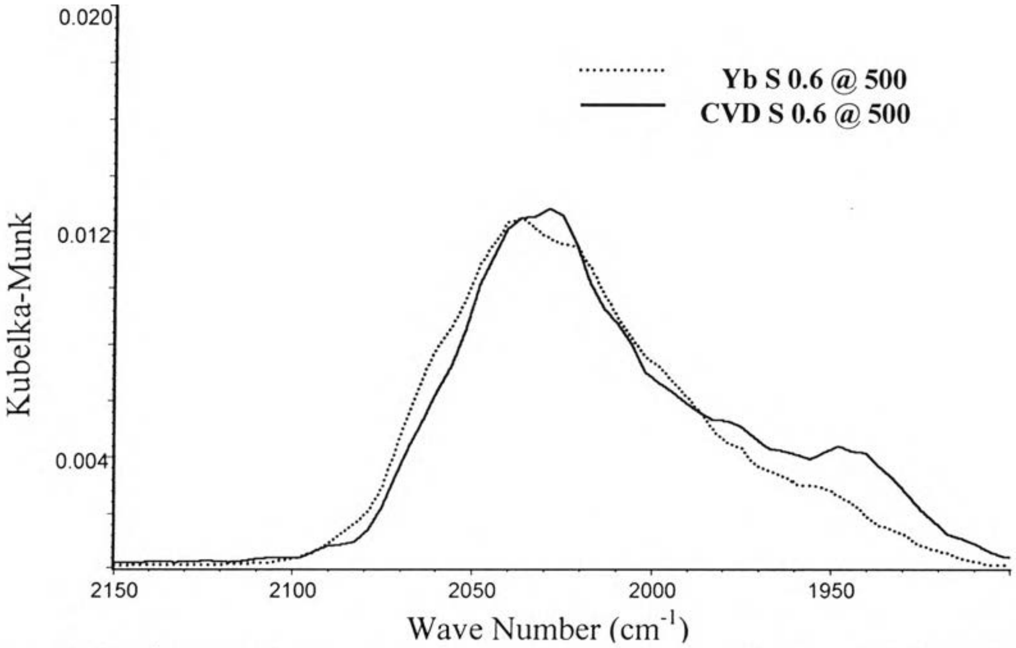

Figure 4.10 The FTIR spectra of adsorbed CO on Pt/KL and PtYb/KL prepared by CVD method after spent in 0.6 ppm sulfur and reduction at 500°C.

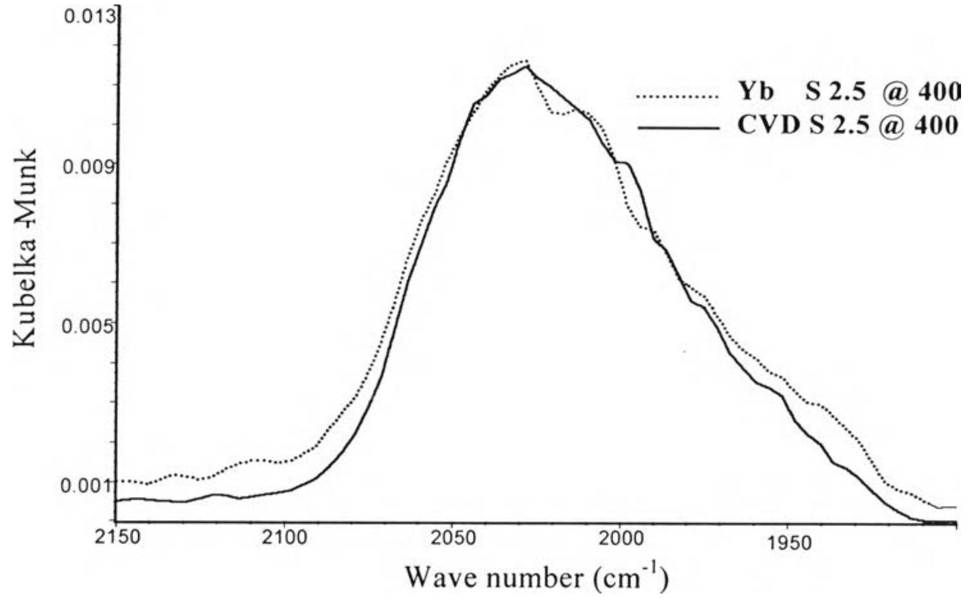

Figure 4.11 The FTIR spectra of adsorbed CO on Pt/KL and PtYb/KL prepared by CVD method after spent in 2.5 ppm sulfur and reduction at 400°C.

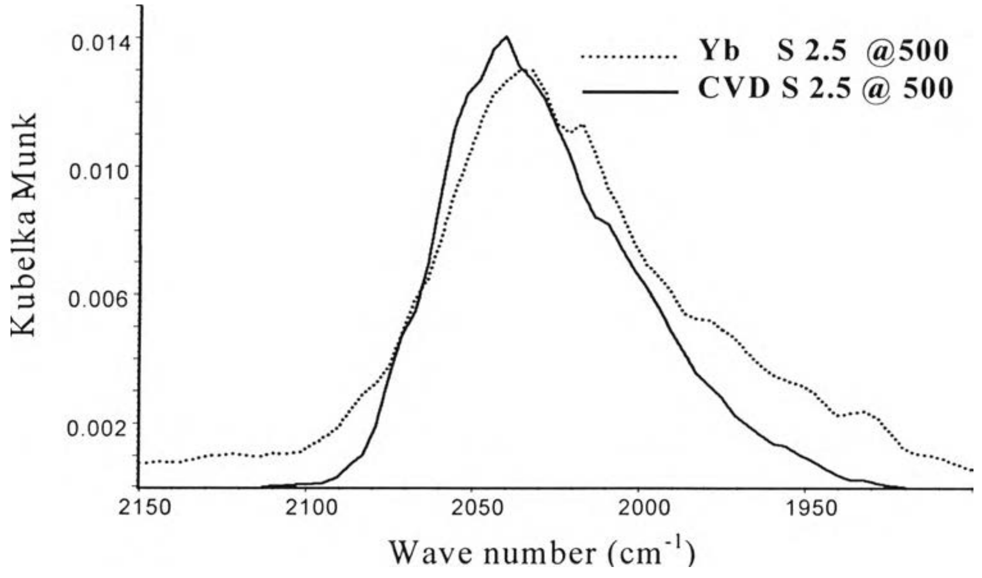

Figure 4.12 The FTIR spectra of adsorbed CO on Pt/KL and PtYb/KL prepared by CVD method after spent in 2.5 ppm sulfur and reduction at 500°C.

4.2 Catalytic Activity Testing

The complete interpretation of the catalytic properties of all catalysts lies on the characterization that provides the evidence of the catalyst morphology and the catalytic performance testing that provided the activity and stability of the catalyst. Therefore the n-hexane aromatization reaction in flow reactor at WHSV = 5 hr^{-1} was also studied at 400 °C and 500°C.

The results and discussion in this section can be divided into three parts: (I) Effect of preparation method, (II) Effect of Ytterbium to the activity and selectivity of Pt/KL and (III) Effect of sulfur to the catalytic activity and selectivity of the catalysts.

4.2.1 Effect of Preparation Method

This part is the comparison between Pt/KL catalysts that were prepared by incipient wetness impregnation (IWI) method and chemical vapor deposition (CVD) method which the Pt precursors were introduced in the liquid and vapor phase, respectively. The reaction had been investigated in the absence of sulfur at the reduction and reaction temperature at 400 °C and 500°C. In the n-hexane aromatization, all catalysts showed the high benzene selectivity around 60-80% for both temperatures (Figure 4.13).

CVD catalysts showed the higher benzene selectivity and n-hexane conversion (Figures 4.13 and 4.14) than IWI catalysts at either 400°C or 500°C. A much lower conversion of IWI catalysts than CVD catalysts at 500°C in comparison with at 400°C illustrated that the activity of IWI catalyst was decreased at high temperature confirming the FTIR results, which demonstrated the high sensitivity to extremely high temperature of IWI catalyst.

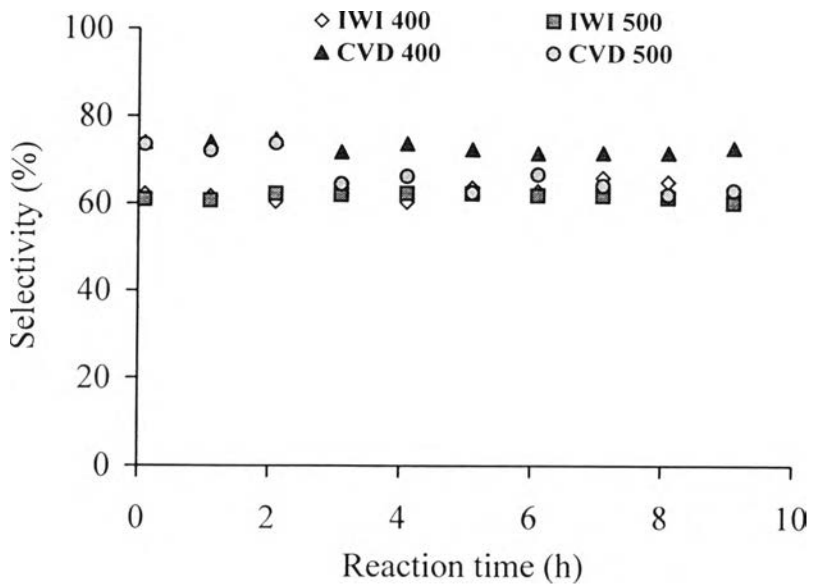

Figure 4.13 The selectivity of Pt/KL prepared by IWI and CVD methods at 400 °C and 500 °C.

The EXAFS, MCP-ring opening and TEM experiments performed by Jacobs *et al.*(1999) showed that the IWI procedure incorporated small cluster into the L-zeolite. It appeared that after preparation, a fraction of the cluster was in close proximity with one another. This fraction of small particles located near the mouth of pore, agglomerated to fill and partially block the channels. Their conclusion agrees with the FTIR results in this work which showed the obvious bands around 2050 cm^{-1}.

Therefore it implies that CVD catalysts have higher thermal stability than IWI catalysts due to the high dispersion of Pt particles from vapor phase impregnation method. Significantly, the CVD catalysts gave the higher benzene yields than IWI catalyst as showed in Figure 4.15.

Hexenes are the primary products of Pt/KL, the monofunctional catalyst (Manninger *et al.*, 1990).The conversion of hexenes to benzene can be generated from small Pt particles encage in the channel system of L-zeolite. However, at the high conversion such as at high temperature or low WHSV, the probability to convert hexenes to benzene was increased (Manninger *et al.*, 1990). The low amount of hexenes may indicate it's enhancing reactivity in aromatization.

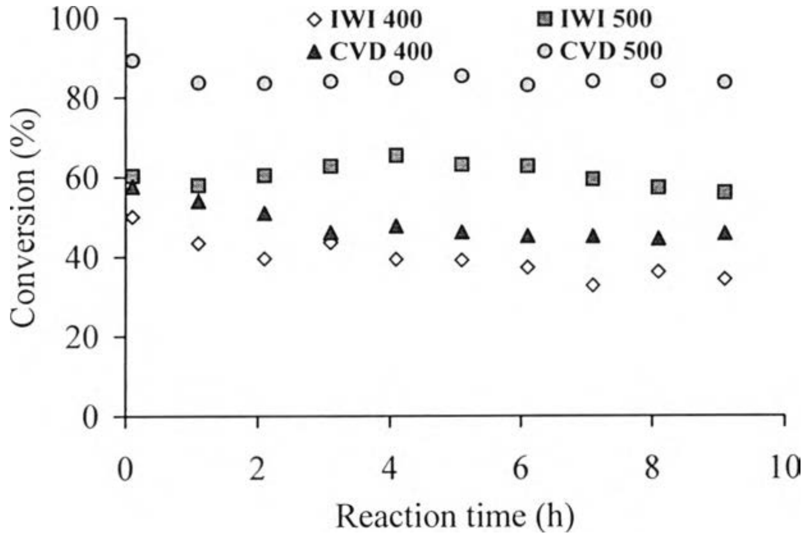

Figure 4.14 The conversion of Pt/KL prepared by IWI and CVD methods at 400 °C and 500 °C.

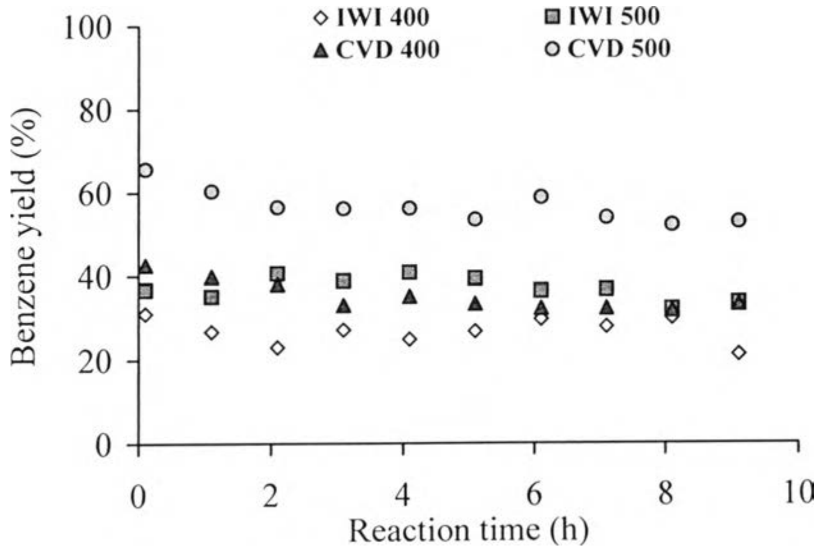

Figure 4.15 The benzene yield of Pt/KL prepared by IWI and CVD methods at 400 °C and 500 °C.

Hexenes yield can also be used as an indicator of the loss of aromatization activity, in the case of hexenes that were produced from the large Pt cluster outside the zeolite channels (Jacobs *et al.*, 1998). The large amount of hexenes yield obtained from IWI catalysts in the Figure 4.16 at 500 °C indicated that the high reduction and reaction temperature could cause the loss in the aromatization activity of IWI catalysts. This can be confirmed by FTIR spectrum that reveals the evidence of the major Pt cluster outside the channels of zeolites in IWI catalyst.

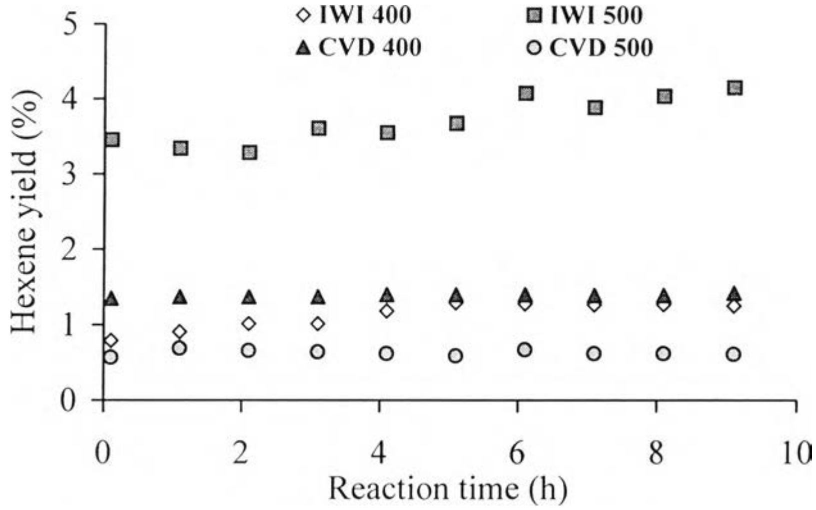

Figure 4.16 The hexenes yield of Pt/KL prepared by IWI and CVD methods at 400 °C and 500 °C.

As mentioned above, it can be concluded that CVD preparation method is more preferable than IWI method. The reasons are as follows:

1. The catalyst that was prepared by CVD method has smaller particles than the catalyst that was prepared by IWI method.

2. The CVD catalysts have higher fraction of Pt particles located inside the channels of zeolite than IWI catalysts.

The important description for the advantage of CVD method is that Pt particles in CVD catalysts are small enough to allow for the diffusion of reactants and products around the cluster during the aromatization of of reactants and products around the cluster during the aromatization of n-hexane, thus resulting in the high activity and selectivity.

Moreover, their EXAFS information ascribed that CVD catalyst displayed the lower Pt-Pt coordination and higher Pt coordination to L-zeolite oxygen atoms in comparison with IWI catalyst.

All of reasons above resulted in the high catalytic selectivity, activity and stability of CVD catalysts. From these experiments, the CVD methods showed the greater ability than IWI method so CVD method was selected for loading metals in the preparation of ytterbium promoted catalyst.

4.2.2 Effect of Ytterbium on Activity and Selectivity of Pt/KL

This part is the comparison in the catalytic performance between the unpromoted catalyst (Pt/KL) and ytterbium promoted catalyst (PtYb/KL) that was prepared by CVD method.

From Figure 4.17, PtYb/KL had the selectivity as high as Pt/KL catalyst at both temperatures. It indicated that the addition of ytterbium did not change the property in high selectivity of Pt/KL catalyst. However, at 500°C PtYb/KL showed the higher conversion than Pt/KL at the initial stage (Figure 4.18). This can be described with FTIR spectrum that PtYb/KL have sensitive to thermal treatment (Figure 4.21). Unfortunately, at 400°C PtYb/KL has lower conversion than Pt/KL. This may be due to the slow adsorption of reactant on active site at low thermodynamic environment. Ytterbium may have some undesirable effect on the adsorption of n-hexane on Pt, resulting in the low conversion of PtYb/KL at 400°C.

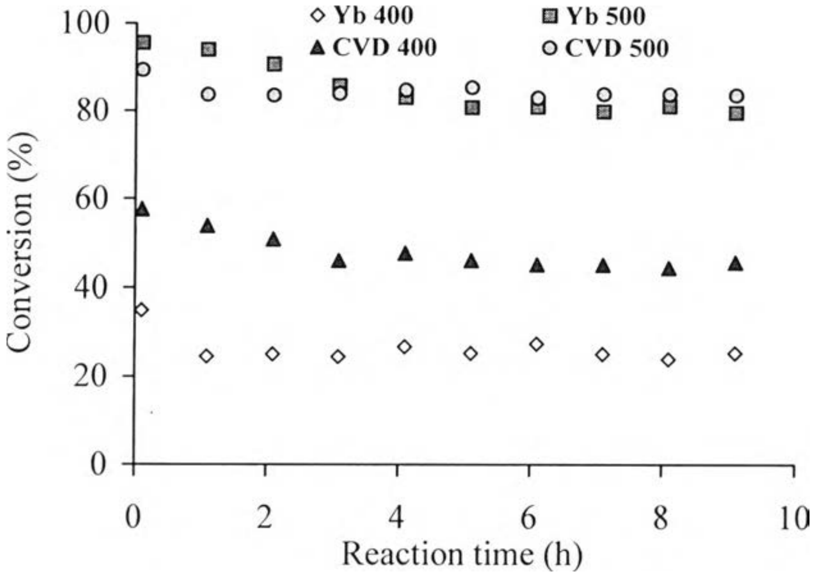

Figure 4.17 The selectivity of Pt/KL and PtYb/KL at 400 °C and 500 °C.

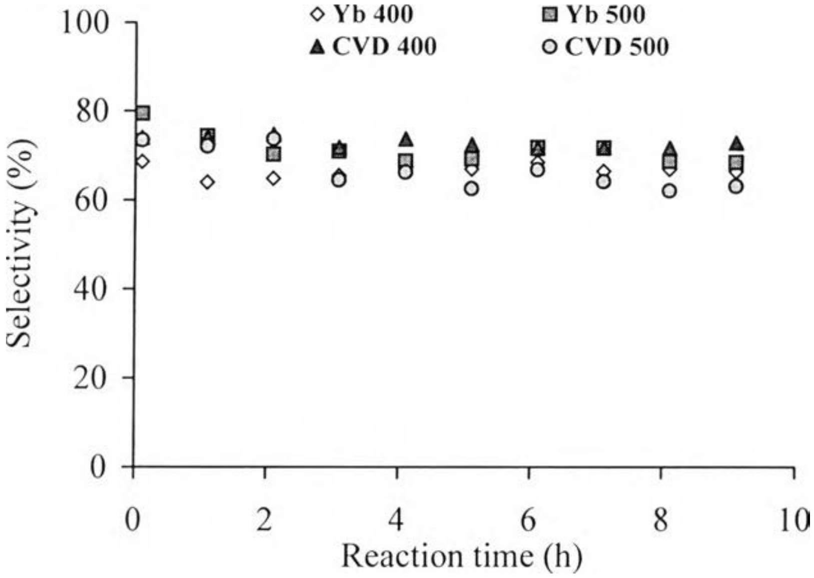

Figure 4.18 The conversion of Pt/KL and PtYb/KL at 400 °C and 500 °C.

According to the selectivity and the conversion of catalysts, PtYb/KL had higher benzene yield than Pt/KL in the initial of reaction at 500°C. Otherwise PtYb/KL had lower benzene yield than Pt/KL at 400°C (Figure 4.19). With the more smaller cluster reside in the channel, PtYb/KL produced less hexenes than Pt/KL as shown in Figure 4.20.

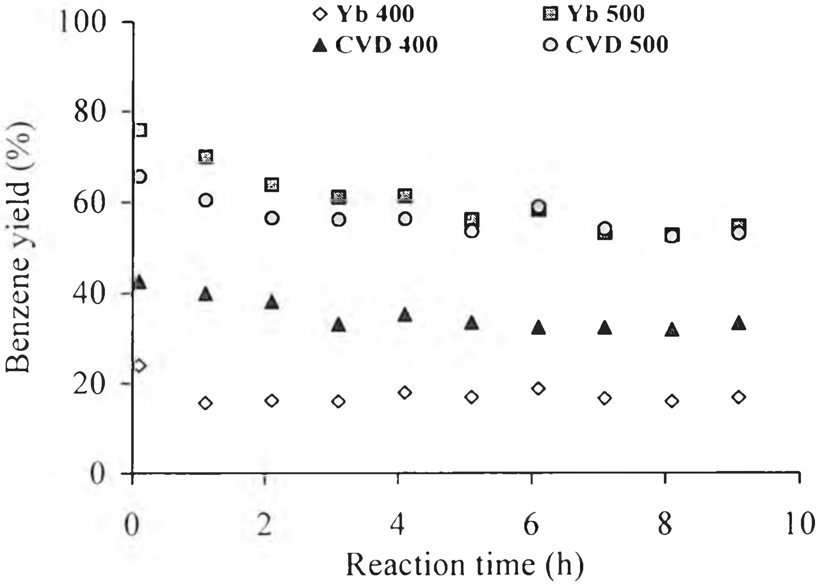

Figure 4.19 The benzene yield of Pt/KL and PtYb/KL at 400 °C and 500 °C.

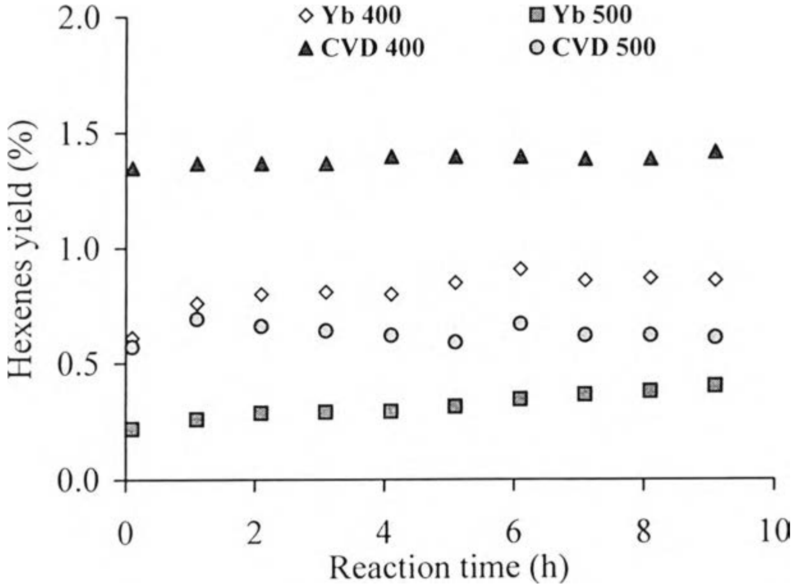

Figure 4.20 The hexenes yield of Pt/KL and PtYb/KL at 400 °C and 500 °C.

Therefore the critical property of ytterbium promoted catalyst is the great dispersion of small Pt particles that located inside the channels of zeolite. It is illustrated from the minor amount of hexenes that typically produced from the large cluster outside the channels when ytterbium promoted to the catalysts. This conforms with FTIR spectra of adsorbed CO at low frequency in Figures 4.7 and 4.8 as previously demonstrated that Pt cluster in PtYb/KL have small size located inside the channels of L-zeolite.

The reason of the high degree dispersion of PtYb/KL can be described that ytterbium oxide was not reduced at this temperature and it can penetrate between the Pt particles resulting in the increase in Pt dispersion (Fang *et al.*,1997).

The drop in the selectivity and conversion of PtYb/KL after 4-5 h to the similar conversion with that of Pt/KL can be described by Figure 4.21.

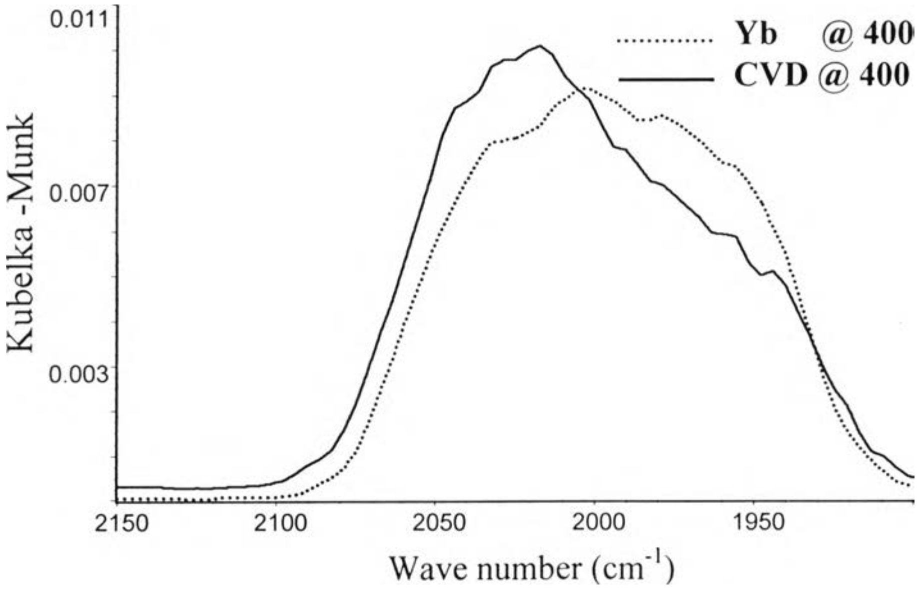

Figure 4.21 The FTIR spectra of adsorbed CO on PtYb/KL after reduction at 400 °C and 500 °C.

From Figure 4.21, the shift of the spectra to the higher wave number after reduction at 500 °C demonstrated that the anchoring of ytterbium in the zeolite pore walls might not be strong enough. Therefore ytterbium oxides were removed from the surface and could block some part of channels and thus reduced the catalytic activity of PtYb/KL.

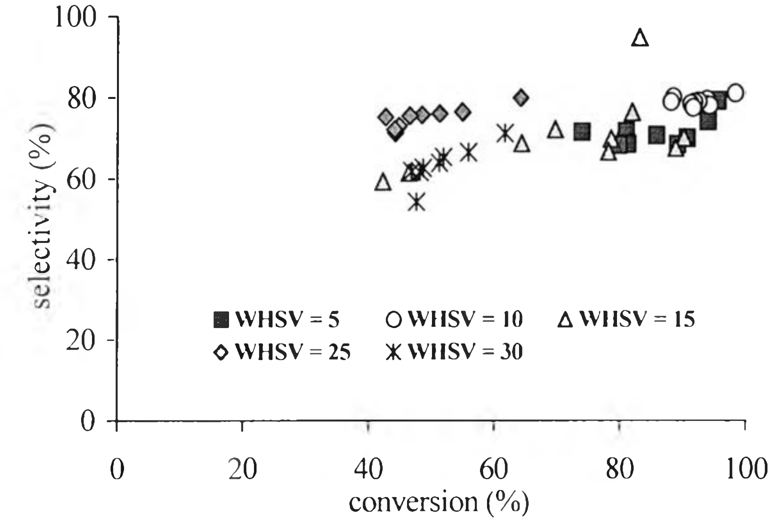

Figure 4.22 The selectivity of PtYb/KL at different % conversions and various WHSV (h^{-1}) at 500 °C.

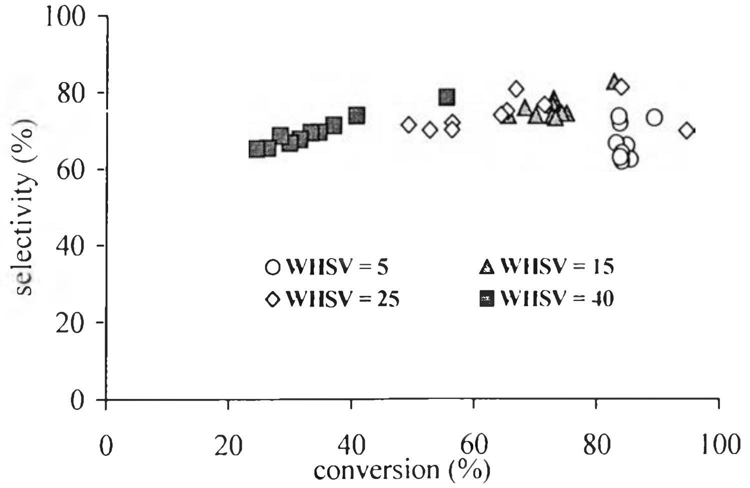

Figure 4.23 The selectivity of Pt/KL at different % conversions and various WHSV (h^{-1}) at 500 °C.

Figures 4.22 and 4.23 showed the important property of PtYb/KL and Pt/KL, respectively, which was the high selectivity even at low conversion.

4.2.3 Effect of Sulfur on Catalytic Activity and Selectivity

This is the most important part because sulfur poisoning is the main cause of Pt/KL deactivation. The scrutiny in the stability of catalysts to the sulfur poisoning is necessary. Thiophene was used as a source of sulfur when it decomposed. Thiophene was mixed with n-hexane to receive the sulfur concentration of 0.6 ppm and 2.5 ppm. The Pt/KL and PtYb/KL prepared by CVD method were selected to study because both of them remarked better properties than IWI catalyst in the absence of sulfur. In the presence of sulfur, the catalysts may show their difference in the sulfur tolerance.

4.2.3.1 Effect of Sulfur 0.6 ppm

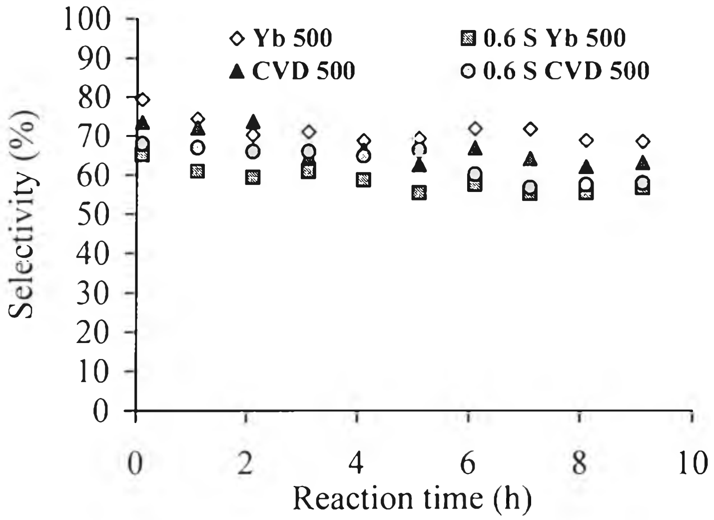

Figure 4.24 The selectivity of Pt/KL and PtYb/KL under 0.6 ppm sulfur condition at 500 °C.

At 500°C, in the presence of 0.6 ppm sulfur, the selectivity of Pt/KL and PtYb/KL were slightly decreased as shown in Figure 4.24.

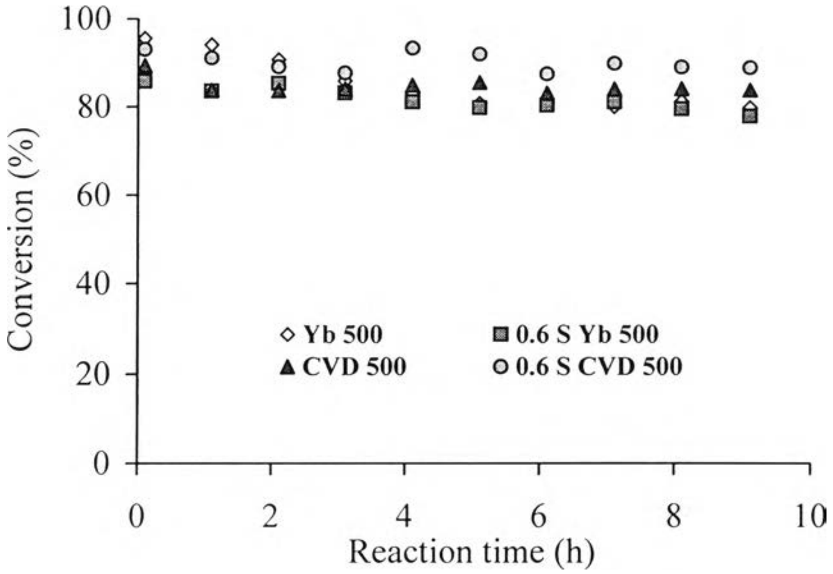

Figure 4.25 The conversion of Pt/KL and PtYb/KL under 0.6 ppm sulfur condition at 500 °C.

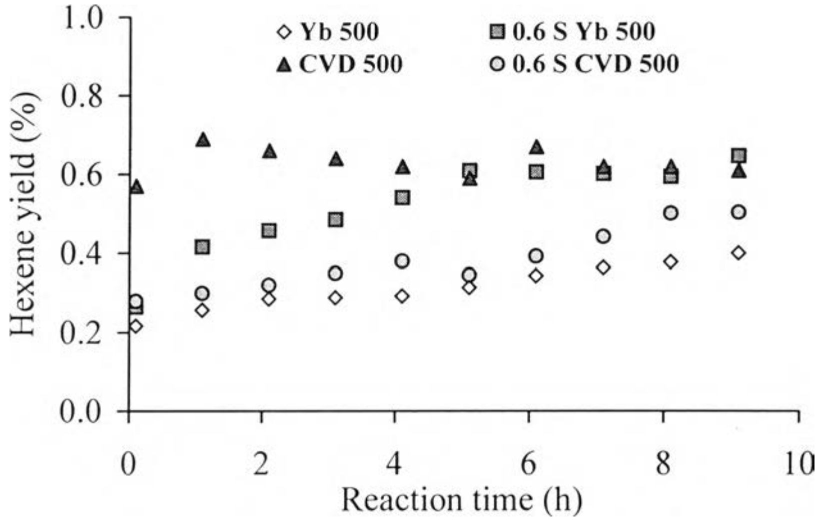

Figure 4.26 The hexenes yield of Pt/KL and PtYb/KL under 0.6 ppm sulfur condition at 500 °C.

The conversion of the n-hexane in Figure 4.25 was not significantly changed when compared with the catalysts in the absence of sulfur. It can be presumed that Pt/KL and PtYb/KL catalyst prepared by CVD method have the sulfur tolerance under the reaction conditions due to the minor of active sites were poisoned. However, the increasing in amount of hexenes yield predicted that the catalysts had some ensemble of Pt particles and would migrate out of the pore thus loosing their characteristics or would block the channels in the longer reaction time.

From Figure 4.26, the poisoned Pt/KL had lower hexenes yield than the poisoned PtYb/KL. This was due to the poisoning by sulfur of Pt cluster outside the pore before the cluster inside the pore. In the case of PtYb/KL, sulfur preferred to poison ytterbium more than Pt because rare earth elements had stronger positive charge than Pt thus it could act as sulfur getter (Jacobs *et al.*, 1999). Consequently, the amount of hexenes from poisoned PtYb/KL received from both large Pt cluster inside and outside the channels of KL-zeolite.

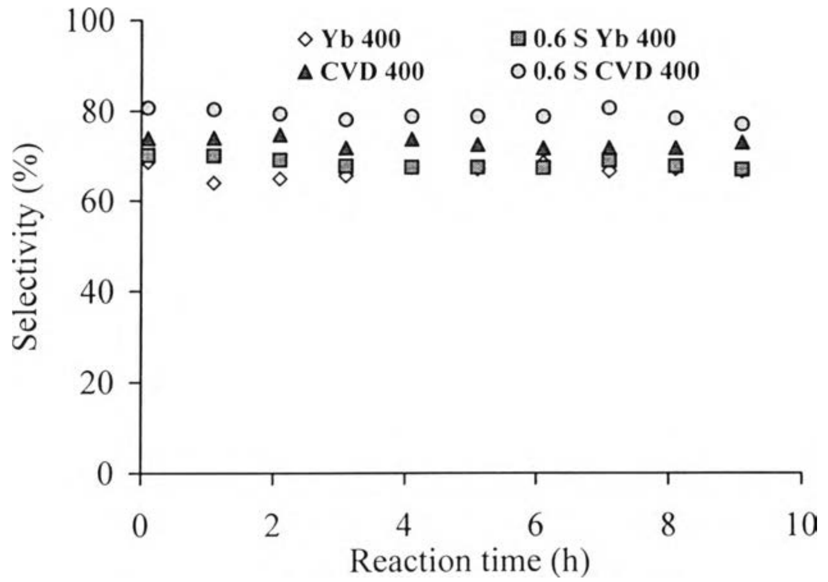

Figure 4.27 The selectivity of Pt/KL and PtYb/KL under 0.6 ppm sulfur condition at 400 °C.

The selectivity and the conversion of Pt/KL and PtYb/KL catalysts in the presence of 0.6 ppm sulfur at 400 °C was shown in Figures 4.27 and 4.28, respectively. The selectivity of poisoned catalyst rarely changed but the conversion from Pt/KL and PtYb/KL catalyst significantly increased in the presence of sulfur (Figure 4.28). It can be assumed that the poisoned of the Pt particles outside the channels by sulfur might increase the catalytic activity of Pt/KL and PtYb/KL.

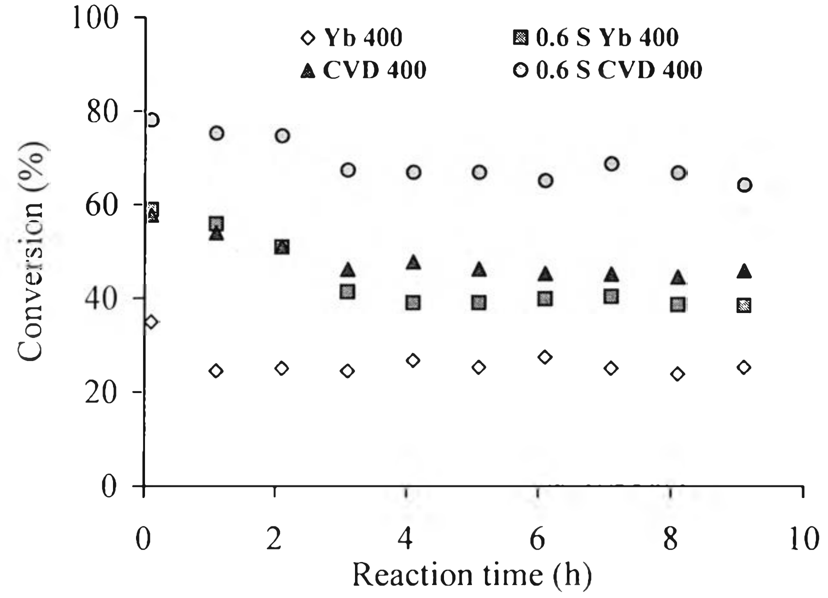

Figure 4.28 The conversion of Pt/KL and PtYb/KL under 0.6 ppm sulfur condition at 400 °C.

The sulfur poisoning of Pt particles resulted in the decrease in hexenes yield as observed in Figure 4.29.

To investigate the role of ytterbium in the sulfur tolerance of Pt/KL, experiments under higher sulfur concentration were done. Sulfur concentration of 2.5 ppm that is higher than the real application was chosen.

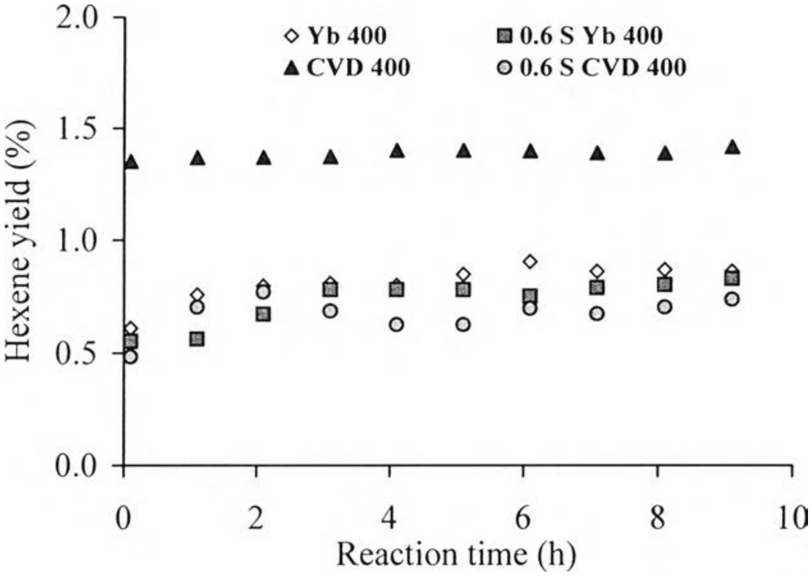

Figure 4.29 The hexenes yield of Pt/KL and PtYb/KL under 0.6 ppm sulfur condition at 400 °C.

4.2.3.2 Effect of Sulfur 2.5 ppm

At 500°C, the results in the sulfur tolerance of Pt/KL and PtYb/KL were similar to the results for 0.6 ppm sulfur but the deactivation of catalysts was clearly be observed. PtYb/KL had higher deactivation rate than Pt/KL as indicated by the lower selectivity, conversion, benzene yield and higher hexenes yield than Pt/KL (Figures 4.30 – 4.32). The deactivation of PtYb/KL at 500°C may be occurred from the low ability of ytterbium to anchoring in the pore system of L-zeolite at higher temperatures. This assumption can be observed from the high catalytic performance of PtYb/KL in the initial reaction time, both under free-sulfur and sulfur conditions.

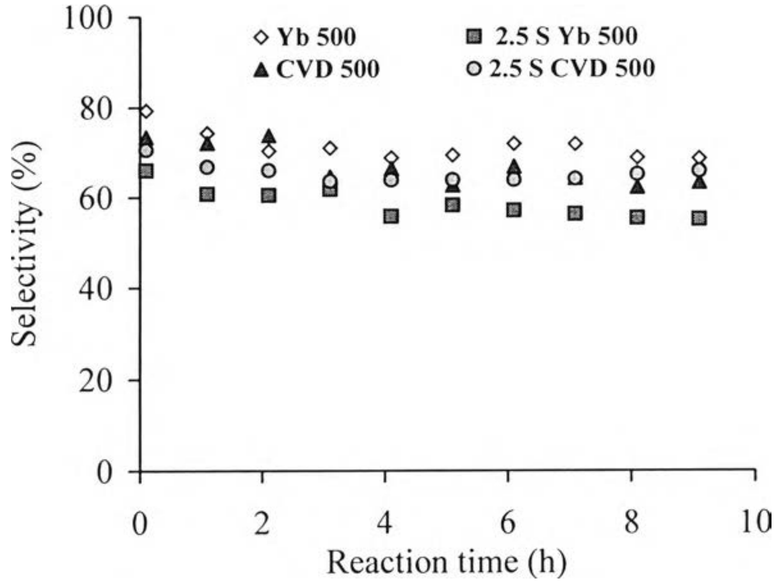

Figure 4.30 The selectivity of Pt/KL and PtYb/KL under 2.5 ppm sulfur condition at 500 °C.

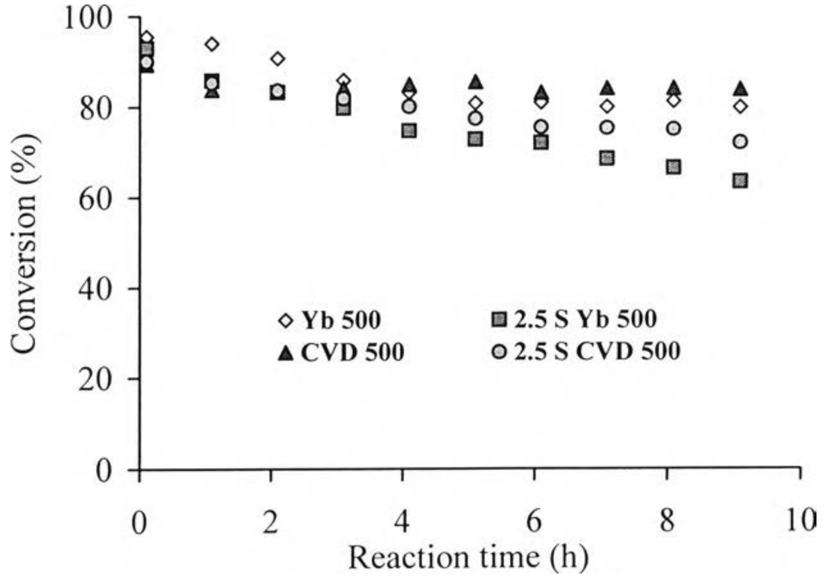

Figure 4.31 The conversion of Pt/KL and PtYb/KL under 2.5 ppm sulfur condition at 500 °C.

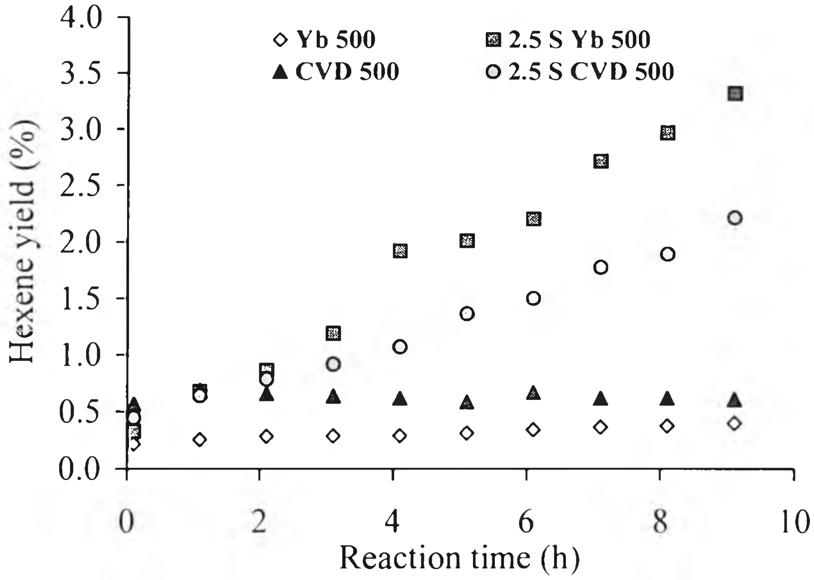

Figure 4.32 The hexenes yield of Pt/KL and PtYb/KL under 2.5 ppm sulfur condition at 500 °C.

At 400°C, for 2.5 ppm sulfur concentration, the benzene selectivity did not change (Figure 4.33). In addition, the poisoned PtYb/KL had higher n-hexane conversion and benzene yield than the poisoned Pt/KL (Figure 4.34 and 4.35). Thus it can be summarized that ytterbium performed better in the presence of sulfur at 400°C. However, the increasing in hexenes yield of poisoned PtYb/KL as seen in Figure 4.36 indicated that the Pt cluster began to grow after all of ytterbium was poisoned. PtYb/KL should be further investigated using the longer reaction time.

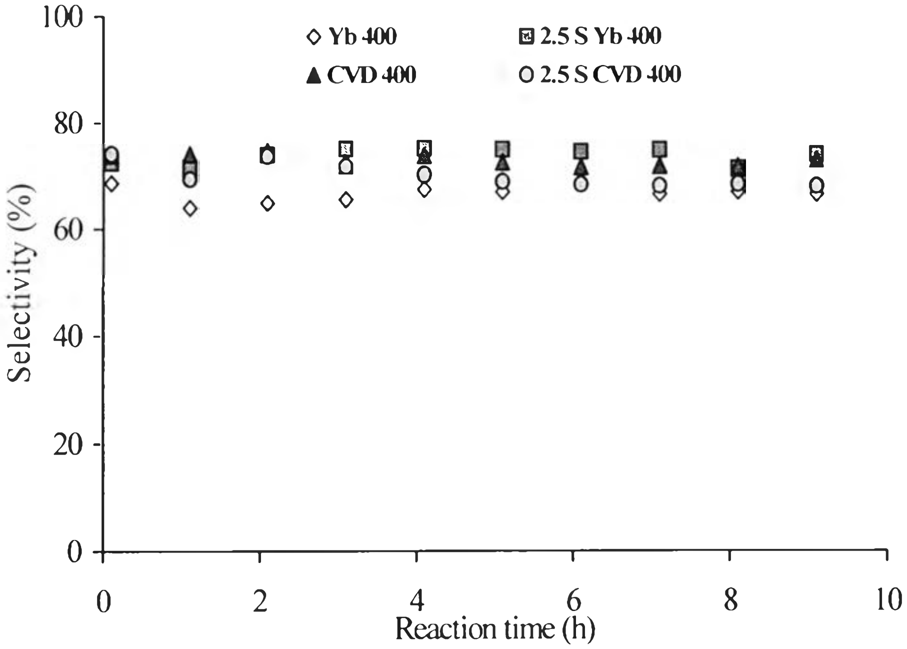

Figure 4.33 The selectivity of Pt/KL and PtYb/KL under 2.5 ppm sulfur condition at 400 °C.

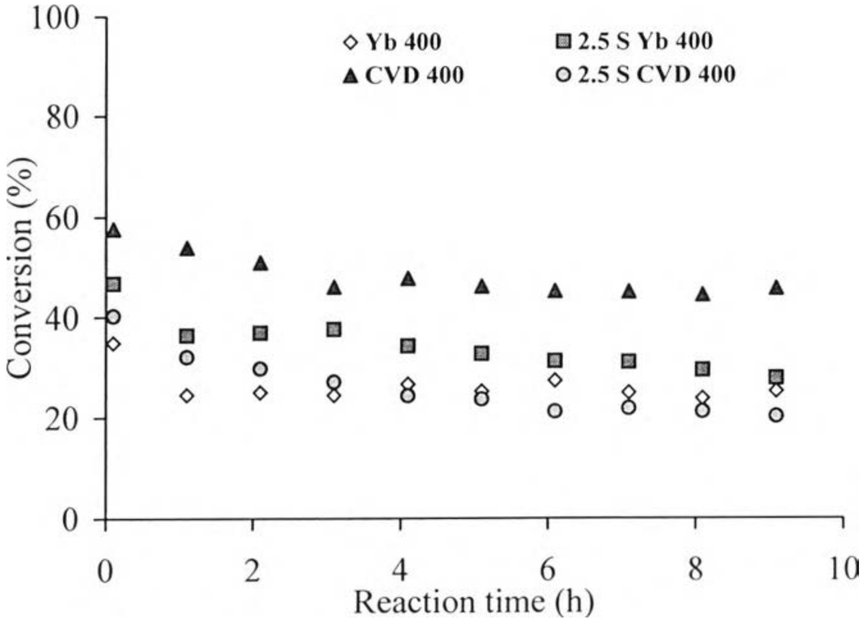

Figure 4.34 The conversion of Pt/KL and PtYb/KL under 2.5 ppm sulfur condition at 400 °C.

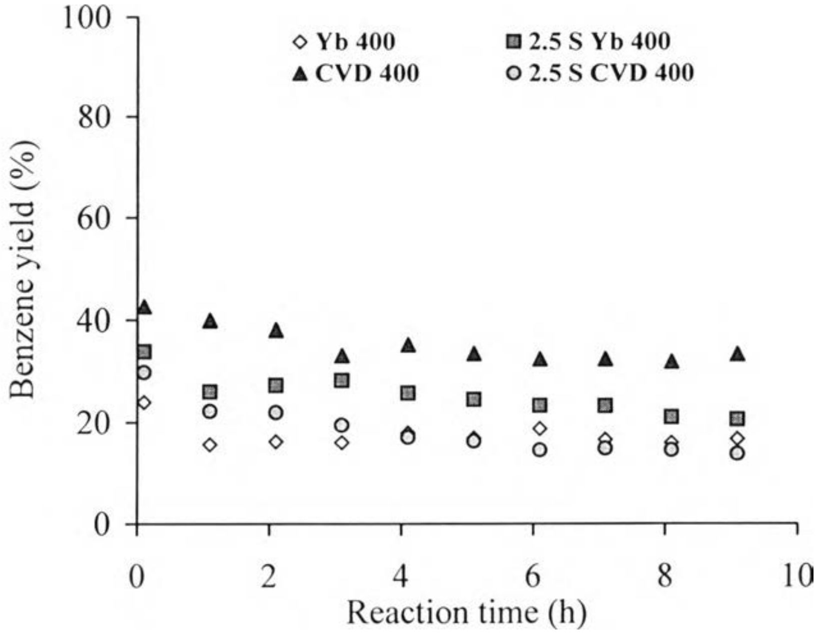

Figure 4.35 The benzene yield of Pt/KL and PtYb/KL under 2.5 ppm sulfur condition at 400 °C.

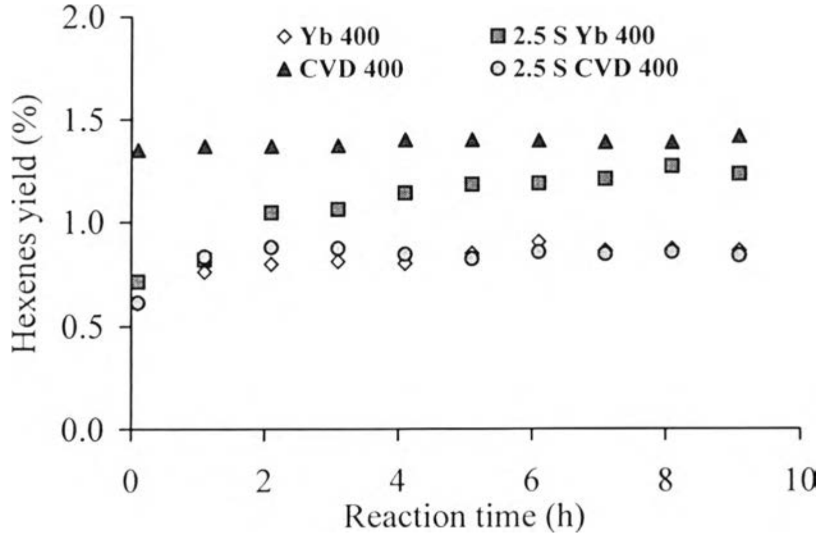

Figure 4.36 The hexenes yield of Pt/KL and PtYb/KL under 2.5 ppm sulfur condition at 400 °C